

Remarks on the state of the art of a posteriori error control of elliptic PDEs in energy norms in practise

Carsten Carstensen and Christian Merdon

Abstract. Five classes of up to 9 a posteriori error estimators compete in three second-order model problems, namely the conforming and non-conforming first-order approximation of the Poisson-Problem plus some conforming obstacle problem. Our numerical results provide sufficient evidence that guaranteed error control in the energy norm is indeed possible with efficiency indices between one and three. The five classes of error estimator consist of the standard residual-based error estimators, averaging error estimators, equilibration error estimators, e.g. the ones of Braess or Luce and Wohlmuth, least-square error estimators and the localisation error estimator of Carstensen and Funken. For the error control for obstacle problems, Braess considers Lagrange multipliers and some resulting auxiliary equation to view the a posteriori error control of the error in the obstacle problem as computable terms plus errors and residuals in the auxiliary equation. Hence all the former a posteriori error estimators apply to this benchmark as well and lead to surprisingly accurate guaranteed upper error bounds. This approach allows an extension to more general boundary conditions and a discussion of efficiency for the affine benchmark examples. The Luce-Wohlmuth and the least-square error estimators win the competition in several computational benchmark problems. Novel equilibration of nonconsistency residuals and novel conforming averaging error estimators win the competition for Crouzeix-Raviart nonconforming finite element methods. Furthermore, accurate error control is slightly more expensive but pays off in all applications under consideration while adaptive mesh-refinement is sufficiently pleasant as accurate when based on explicit residual-based error estimates.

Mathematics Subject Classification (2010): 65N30, 65R20, 73C50.

Keywords: A posteriori error estimators, finite element methods.

This work was supported by DFG Research Center MATHEON and by the World Class University (WCU) program through the National Research Foundation of Korea (NRF) funded by the Ministry of Education, Science and Technology R31-2008-000-10049-0. The second author was also supported by the German Academic Exchange Service (DAAD, D/10/44641) during his stay at the Yonsei University in 2010.

1. Introduction

A posteriori finite element error control for second-order elliptic boundary value problems involves the computation of guaranteed upper bounds of some residual Res in the dual $H^{-1}(\Omega)$ of $H_0^1(\Omega)$ with respect to the dual norm. The majority of applications in computational PDEs [19, 20] applies to the residual

$$\text{Res}(v) = \int_{\Omega} (fv - \sigma_h \cdot Dv) \, dx$$

with some given Lebesgue integrable functions f and σ_h . Traditional equilibration techniques compute some $q \in H(\text{div}, \Omega)$ such that (via an integration by parts) the residual becomes

$$\text{Res}(v) = \int_{\Omega} (f + \text{div } q)v \, dx + \int_{\Omega} (q - \sigma_h) \cdot Dv \, dx$$

and leads to the error estimate

$$\| \text{Res} \|_* := \sup_{v \in H_0^1(\Omega)} \text{Res}(v) / \|v\| \leq \eta(q) := \|f + \text{div } q\|_* + \|q - \sigma_h\|_{L^2(\Omega)}.$$

This paper concentrates on three model problems to support the observation of published and ongoing error estimator competitions [11, 22, 24, 23] that accurate error control is possible with efficiency between 1 and 2. Section 2 introduces the setting for the Poisson model problem and Section 3 recalls the five classes of error estimators from Table 1 to control $\| \text{Res} \|_*$.

TABLE 1. Classes of a posteriori error estimators used in this paper.

No	Classes of error estimators	Class representatives
1	explicit residual-based	η_R
2	averaging	η_{MP1}, η_{A1}
3	equilibration	$\eta_B, \eta_{MFEM}, \eta_{LW}, \eta_{EQL}$
4	least-square	η_{LS}
5	localisation	η_{CF}

Subsection 4.1 explains our adaptive mesh-refinement algorithm. In this paper the adaptive mesh-refinement is driven by local error estimator contributions from any estimator from Table 1 to observe that mesh refinement with the standard residual-based error estimator η_R is suitable and does not need to be replaced by any other marking strategy.

Section 5 deals with nonconforming Crouzeix-Raviart approximations u_{CR} for the Poisson model problem. The Helmholtz decomposition allows a split of the error in the broken energy norm into

$$\|e\|_{NC}^2 \leq \eta^2 + \| \text{Res}_{NC} \|_*^2.$$

The first term η on the right-hand side involves contributions of the right-hand side f and is directly computable (up to quadrature errors). The second

term in the upper error bound is the dual norm of some residual Res_{NC} that enjoys Galerkin orthogonality properties,

$$\|\text{Res}_{\text{NC}}\|_* = \min_{\substack{v \in H^1(\Omega) \\ v = u_D \text{ on } \partial\Omega}} \|\nabla_{\text{NC}} u_{\text{CR}} - \nabla v\|_{L^2(\Omega)}.$$

Upper bounds of $\|\text{Res}_{\text{NC}}\|_*$ are computed by the error estimators of Table 1 or by the design of some $v \in H^1(\Omega)$ with Dirichlet data $v = u_D$ along $\partial\Omega$.

Section 6 extends applications to obstacle problems with affine obstacles by introduction of some auxiliary Poisson problem after [12].

2. Model Poisson problem

This section specifies the setting in the Poisson model problem.

2.1. Discrete problem

Given a bounded Lipschitz domain Ω and right-hand side $f \in L^2(\Omega)$, the Poisson model problem seeks the exact solution $u \in H^1(\Omega)$ with $u = 0$ along $\partial\Omega$ and

$$-\Delta u = f \text{ in } \Omega.$$

Given a regular triangulation \mathcal{T} of $\Omega \subseteq \mathbb{R}^2$ into triangles with edges \mathcal{E} , nodes \mathcal{N} , and free nodes \mathcal{K} , let $P_k(T)$ denote the polynomials of degree $\leq k$ on $T \in \mathcal{T}$ and

$$P_k(\mathcal{T}) := \{v_h \in L^2(\Omega) \mid \forall T \in \mathcal{T}, v_h|_T \in P_k(T)\}.$$

The first-order Courant finite element method computes the discrete solution $u_h \in V(\mathcal{T}) := P_1(\mathcal{T}) \cap C_0(\Omega)$ with gradient $\sigma_h := \nabla u_h$ as

$$\int_{\Omega} \nabla u_h \cdot \nabla v_h \, dx = \int_{\Omega} f v_h \, dx \quad \text{for all } v_h \in V(\mathcal{T}). \tag{2.1}$$

2.2. Residual

The related residual $\text{Res} \in V^*$ is a linear and bounded functional

$$\text{Res}(v) := \int_{\Omega} f v \, dx - \int_{\Omega} \sigma_h \cdot \nabla v \, dx$$

for the Sobolev functions v in the Hilbert space $V := H_0^1(\Omega)$ endowed with the (semi-) norm $\|\cdot\| := \|\nabla \cdot\|_{L^2(\Omega)}$. It is clear from the Riesz representation theorem that the energy norm $\|e\|$ of the error $e := u - u_h$ equals the norm of $\|\text{Res}\|_*$ of the residual Res (cf., e.g., [15, Section 5.1.2, p. 86] and [20, Section 3.3]). A posteriori equilibration error estimators derive computable upper bounds of $\|\text{Res}\|_*$ through the introduction of some equilibrated $q \in H(\text{div}, \Omega)$. An integration by parts shows

$$\text{Res}(v) = \int_{\Omega} (f + \text{div } q)v \, dx + \int_{\Omega} (q - \sigma_h) \cdot \nabla v \, dx$$

and therefore leads to

$$\|\text{Res}\|_* \leq \|f + \text{div } q\|_* + \|q - \sigma_h\|_{L^2(\Omega)}.$$

The equilibration error estimator of Braess [13, 26] is one modern example for a proper choice of q in $RT_0(\mathcal{T}) \subseteq H(\operatorname{div}, \Omega)$,

$$RT_0(\mathcal{T}) := \left\{ q(x) = a_{\mathcal{T}}x + (b_{\mathcal{T}}, c_{\mathcal{T}}) \in H(\operatorname{div}, \Omega) \mid a_{\mathcal{T}}, b_{\mathcal{T}}, c_{\mathcal{T}} \in P_0(\mathcal{T}) \right\}.$$

Earlier examples of Ladeveze [29, 3] and [21] also provide a source of a posteriori error estimators compared in [11, 22]. If the local problems therein are solved exactly, they also yield guaranteed upper bounds. It is unrealistic to assume an exact solve of those local problems in practise and so the displayed numbers in [21, 11, 22] are only lower bounds for the guaranteed upper bounds. This fundamental difficulty is circumvented by modern equilibration error estimators, like the ones of Braess and Luce-Wohlmuth.

2.3. Inhomogenous Dirichlet boundary conditions

In case of inhomogenous boundary conditions $u = u_D$ along the boundary edges $\mathcal{E}(\partial\Omega) := \{E \in \mathcal{E} \mid E \subset \partial\Omega\}$, the discrete solution u_h satisfies $u_h = \mathcal{I}u_D := \sum_{z \in \mathcal{N}} u_D(z)\varphi_z$. Since $e = u - u_h = u_D - \mathcal{I}u_D \notin H_0^1(\Omega)$, the equation $\|e\| = \|\operatorname{Res}\|_*$ does not hold.

Theorem 2.1. *Assume that $u_D \in H^1(\Omega) \cap C(\Omega)$ satisfies $u_D \in H^2(E)$ for all $E \in \mathcal{E}(\partial\Omega)$. Let $\partial_{\mathcal{E}}^2 u_D / \partial s^2$ denote the edgewise second partial derivative of u_D along $\partial\Omega$. Then there exists $w_D \in H^1(\Omega)$ and some constant $C_\gamma \lesssim 1$ (which depends only on the interior angles of \mathcal{T}) with*

$$\begin{aligned} w_D|_{\partial\Omega} &= u_D|_{\partial\Omega} - \mathcal{I}u_D|_{\partial\Omega}, \\ \operatorname{supp}(w_D) &\subset \bigcup \{T \in \mathcal{T} \mid T \cap \partial\Omega \neq \emptyset\}, \\ \|w_D\|_{L^\infty(\Omega)} &= \|u_D - \mathcal{I}u_D\|_{L^\infty(\partial\Omega)}, \\ \|w_D\| &\leq C_\gamma \|h_{\mathcal{E}}^{3/2} \partial_{\mathcal{E}}^2 u_D / \partial s^2\|_{L^2(\partial\Omega)}. \end{aligned}$$

Furthermore it holds

$$\|e\|^2 \leq \|\operatorname{Res}\|_*^2 + \|w_D\|^2.$$

Proof. For the proof of the existence of w_D see [9]. For the proof of the last equation, assume the optimal $w \in H^1(\Omega)$ with $w|_{\partial\Omega} = u|_{\partial\Omega} - \mathcal{I}u|_{\partial\Omega}$ and $\operatorname{div} \nabla w \equiv 0$. Then, it holds the orthogonality from [9],

$$\|e\|^2 = \|e - w\|^2 + \|w\|^2 \leq \|\operatorname{Res}\|_*^2 + \|w\|^2 \leq \|\operatorname{Res}\|_*^2 + \|w_D\|^2.$$

This concludes the proof. □

Remark 2.2. More explicit calculations in [24] show $C_\gamma \leq 0.7043$ for triangulations with right isosceles triangles. However, for the numerical examples in this paper, we use $C_\gamma = 1$.

3. Five types of a posteriori error estimators

This section recalls some representatives of the five classes of error estimators from Table 1.

3.1. Notation

Consider a regular triangulation \mathcal{T} of $\Omega \subseteq \mathbb{R}^2$ into triangles with nodes \mathcal{N} , free nodes $\mathcal{K} := \mathcal{N} \setminus \partial\Omega$, edges \mathcal{E} , Dirichlet boundary edges $\mathcal{E}(\partial\Omega) := \{E \in \mathcal{E} \mid E \subseteq \partial\Omega\}$. Each node z in \mathcal{N} is associated with its nodal basis functions φ_z and node patch $\omega_z := \{\varphi_z > 0\}$ with diameter $h_z := \text{diam}(\omega_z)$. Each triangle $T \in \mathcal{T}$ is the closed convex hull of the set $\mathcal{N}(T)$ of its vertices and associated to its element patch $\omega_T := \bigcup_{z \in \mathcal{N}(T)} \omega_z$. The set $\mathcal{E}(T)$ denotes the edges of T in \mathcal{T} and the set $\mathcal{E}(z)$ denotes all edges connected to $z \in \mathcal{N}$.

3.2. Standard residual error estimator

The standard residual error estimator

$$\eta_R := \|h_{\mathcal{T}} f\|_{L^2(\Omega)} + \left(\sum_{E \in \mathcal{E}} h_E \|[\sigma_h \cdot \nu_E]_E\|_{L^2(E)}^2 \right)^{1/2}$$

is a guaranteed upper bound of $\|u - u_h\|$. In all our examples, \mathcal{T} consists of right isosceles triangles and then the generic reliability constant is even 1, i.e. $\|u - u_h\| \leq \eta_R$ [21]. Here, $[\sigma_h \cdot \nu_E]_E$ denotes the jump of $[\sigma_h \cdot \nu_E]_E$ across $E \in \mathcal{E}$, which is set to zero along any Dirichlet edge $E \in \mathcal{E}(\partial\Omega)$.

3.3. Minimal $P_1(\mathcal{T}; \mathbb{R}^2)$ averaging

The error estimator

$$\eta_{\text{MP1}} := \min_{q \in P_1(\mathcal{T}; \mathbb{R}^2) \cap C(\Omega; \mathbb{R}^2)} \|\sigma_h - q\|_{L^2(\Omega)}$$

shows very accurate results for the Laplace equation, but only yields an upper bound for $\|u - u_h\|$ up to some reliability constant C_{rel} [18], which is *not* displayed and expected to be too large to be competitive. Simple averagings $q_A \in P_1(\mathcal{T}; \mathbb{R}^2)$ compute approximations of η_{MP1} , e.g.

$$\eta_{\text{A1}} := \|\sigma_h - q_{\text{A1}}\|_{L^2(\Omega)} \quad \text{with} \quad q_{\text{A1}}(z) = \int_{\omega_z} \sigma_h \, dx / |\omega_z| \quad \text{for all } z \in \mathcal{N}.$$

3.4. Least-square error estimator

An integration by parts yields, for any $q \in H(\text{div}, \Omega)$ and with elementwise integral mean $f_{\mathcal{T}} \in P_0(\mathcal{T})$, that

$$\begin{aligned} & \int_{\Omega} (\nabla u - \sigma_h) \cdot \nabla v \, dx \\ &= \int_{\Omega} (f - f_{\mathcal{T}}) v \, dx + \int_{\Omega} (f_{\mathcal{T}} + \text{div } q) v \, dx + \int_{\Omega} (\sigma_h - q) \cdot \nabla v \, dx. \end{aligned}$$

After [33, 35, 22], this results in the error estimator

$$\eta_{\text{LS}} := \min_{q \in RT_0(\mathcal{T})} C_F \|f_{\mathcal{T}} + \text{div } q\|_{L^2(\Omega)} + \|\sigma_h - q\|_{L^2(\Omega)} + \text{osc}(f, \mathcal{T}) / \pi$$

with Friedrichs' constant $C_F := \sup_{v \in V \setminus \{0\}} \|v\|_{L^2(\Omega)} / \|v\|$, and oscillations

$$\text{osc}(f, \mathcal{T}) := \|h_{\mathcal{T}}(f - f_{\mathcal{T}})\|_{L^2(\Omega)}.$$

Our interpretation of Repin’s variant (without the oscillation split) reads

$$\eta_{\text{REPIN}} := \min_{q \in RT_0(\mathcal{T})} C_F \|f + \operatorname{div} q\|_{L^2(\Omega)} + \|\sigma_h - q\|_{L^2(\Omega)}.$$

This paper studies the least-square variant η_{LS} rather than Repin’s majorant η_{REPIN} for reasons discussed in [22, Subsection 4.2]. Supercloseness results from [14] show that asymptotically the minimiser q_{LS} equals the gradient q_{MFEM} of the mixed finite element method with lowest-order Raviart-Thomas finite elements $RT_0(\mathcal{T})$. In practise η_{LS} is approximated by a series of least-square problems as in [37].

3.5. Luce-Wohlmuth error estimator

Luce and Wohlmuth [30] suggest to solve local problems around each node on the dual triangulation \mathcal{T}^* of \mathcal{T} and compute some equilibrated quantity q_{LW} . The dual triangulation \mathcal{T}^* connects each triangle center $\operatorname{mid}(T)$, $T \in \mathcal{T}$, with the edge midpoints $\operatorname{mid}(\mathcal{E}(T))$ and nodes $\mathcal{N}(T)$ and so divides each triangle $T \in \mathcal{T}$ into 6 subtriangles of area $|T|/6$.

Consider some node $z \in \mathcal{N}(T)$ and its nodal basis function φ_z^* with the fine patch $\omega_z^* := \{\varphi_z^* > 0\}$ of the dual triangulation \mathcal{T}^* and its neighbouring triangles $\mathcal{T}^*(z) := \{T^* \in \mathcal{T}^* \mid z \in \mathcal{N}^*(T^*)\}$. Since $\sigma_h \in P_0(\mathcal{T})$ is continuous along $\partial\omega_z^* \cap T$ for any $T \in \mathcal{T}$, $q \cdot \nu = \sigma_h \cdot \nu \in P_0(\mathcal{E}^*(\partial\omega_z^*))$ is well-defined on the boundary edges $\mathcal{E}^*(\partial\omega_z^*)$ of ω_z^* . With $f_{T,z} := -\int_T f \varphi_z \, dx / |T^*|$ and the local spaces

$$Q(\mathcal{T}^*(z)) := \{\tau_h \in RT_0(\mathcal{T}^*(z)) \mid \operatorname{div} \tau_h|_{T^*} + f_{T,z} = 0 \text{ on } T^* \in \mathcal{T}^* \text{ with } \mathcal{N}^*(T^*) \cap \mathcal{N}(T) = \{z\} \text{ and } q \cdot \nu = \sigma_h \cdot \nu \text{ along } \partial\omega_z^* \setminus \partial\Omega\},$$

the mixed finite element method solves

$$q|_{\omega_z^*} := \operatorname{argmin}_{\tau_h \in Q(\mathcal{T}^*(z))} \|q_h - \tau_h\|_{L^2(\omega_z^*)}.$$

This choice of the divergence [25] differs from the original one of [30] for an improved bound for $\| \|f + \operatorname{div} q_{\text{LW}} \|_{\star}$ with explicitly known constants, namely

$$\| \|f + \operatorname{div} q_{\text{LW}} \|_{\star} \leq \|h_{\mathcal{T}}(f + \operatorname{div} q_{\text{LW}})\|_{L^2(\Omega)} / \pi.$$

For details cf. [25]. The remaining degrees of freedom permit proper boundary fluxes and

$$\int_{\Omega} q_{\text{LW}} \cdot \operatorname{Curl} \varphi_z^* \, dx = \int_{\Omega} \sigma_h \cdot \operatorname{Curl} \varphi_z^* \, dx \quad \text{for all } z \in \mathcal{N}.$$

Here, Curl denotes the rotated gradient $\operatorname{Curl} v := (-\partial v / \partial x_2, \partial v / \partial x_1)$. Then, the Luce-Wohlmuth error estimator reads

$$\eta_{\text{LW}} := \|\sigma_h - q_{\text{LW}}\|_{L^2(\Omega)} + \|h_{\mathcal{T}}(f + \operatorname{div} q_{\text{LW}})\|_{L^2(\Omega)} / \pi.$$

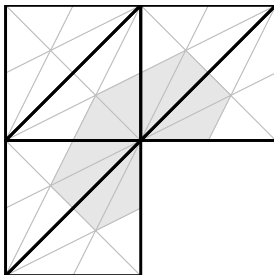


FIGURE 1. Triangulation \mathcal{T} (thick lines), fine triangulation \mathcal{T}^* (thin lines) and ω_z^* (lightgray) around the reentering corner of the L-shaped domain for the Luce-Wohlmuth error estimator.

3.6. Equilibration error estimator by Braess

Braess [13, 26] designs patchwise broken Raviart-Thomas functions $r_z \in RT_{-1}(\mathcal{T}(z))$ that satisfy

$$\begin{aligned} \operatorname{div} r_z|_T &= - \int_T f \varphi_z \, dx / |T| && \text{for } T \in \mathcal{T}(z) \\ [r_z \cdot \nu_E]_E &= -[\sigma_h \cdot \nu_E]_E / 2 && \text{on } E \in \mathcal{E}(z) \cap \mathcal{E}(\partial\Omega) \\ r_z \cdot \nu &= 0 && \text{along } \partial\omega_z \setminus \mathcal{E}(\partial\Omega). \end{aligned}$$

The solution r_z of these problems is unique up to multiplicatives of $\operatorname{Curl} \varphi_z$ and may be chosen such that $\|r_z\|_{L^2(\omega_z)}$ is minimal. Eventually, the quantity $q_B := \sigma_h + \sum_{z \in \mathcal{N}} r_z \in RT_0(\mathcal{T})$ satisfies

$$\operatorname{div} q_B|_T = - \int_T f \, dx / |T|.$$

and allows the dual norm estimate

$$\|f + \operatorname{div} q_B\|_{\star} \leq \operatorname{osc}(f, \mathcal{T}) / \pi.$$

The estimator reads

$$\eta_B := \|\sigma_h - q_B\|_{L^2(\Omega)} + \operatorname{osc}(f, \mathcal{T}) / \pi.$$

3.7. Equilibration error estimator by Ladeveze

The fluxes q_L designed by Ladeveze-Leguillon [29] act as Neumann boundary conditions for local problems on each triangle, cf. also [3] for details. Given the local function space

$$H_D^1(T) = \begin{cases} H^1(T) / \mathbb{R} & \text{if } |T \cap \Gamma_D| = 0 \text{ and else} \\ \{v \in H^1(T) \mid v = 0 \text{ on } \partial T \cap \Gamma_D\}, & \end{cases}$$

seek $\phi_T \in H_D^1(T)$ such that, for all $v \in H_D^1(T)$,

$$\int_T \phi_T \cdot \nabla v \, dx = \int_T f v \, dx - \int_T \sigma_h \cdot \nabla v \, dx + \int_{\partial T} q_L \cdot \nu_T v \, ds.$$

Then the error estimate reads

$$\| \|u - u_h\| \| \leq \eta_{\text{EQL}} := \left(\sum_{T \in \mathcal{T}} \|\nabla \phi_T\|_{L^2(T)}^2 \right)^{1/2}.$$

3.8. Carstensen-Funken error estimator

The partition of unity property of the nodal basis functions ($\varphi_z \mid z \in \mathcal{N}$) leads in [21] to the solution of local problems on node patches ω_z : Seek $w_z \in W_z := \{v \in H_{\text{loc}}^1(\omega_z) \mid \|\varphi_z^{1/2} \nabla v\|_{L^2(\omega_z)} < \infty, v = 0 \text{ on } \partial\Omega \cap \partial\omega_z\}$ if $z \in \mathcal{N}(\partial\Omega)$, or $w_z \in W_z := \{v \in H_{\text{loc}}^1(\omega_z) \mid \|\varphi_z^{1/2} \nabla v\|_{L^2(\omega_z)} < \infty\} / \mathbb{R}$ if $z \in \mathcal{N}(\Omega)$, such that

$$\int_{\omega_z} \varphi_z \nabla w_z \cdot \nabla v \, dx = \int_{\omega_z} \varphi_z f v \, dx - \int_{\omega_z} \sigma_h \cdot \nabla(\varphi_z v) \, dx \quad \text{for all } v \in W_z.$$

Then the error estimator reads

$$\| \|u - u_h\| \| \leq \eta_{\text{CF}} := \left(\sum_{z \in \mathcal{N}} \|\varphi_z^{1/2} \nabla w_z\|_{L^2(\omega_z)}^2 \right)^{1/2}.$$

In the computations for η_{CF} and η_{EQL} , all the local problems are solved with fourth-order polynomials for simplicity. The computed values are regarded as very good approximations. However, strictly speaking the values displayed for η_{EQL} or η_{CF} are lower bounds of the guaranteed upper bounds.

4. Conforming finite element method

4.1. Uniform and adaptive mesh refinement

Automatic mesh refinement generates a sequence of meshes $\mathcal{T}_0, \mathcal{T}_1, \mathcal{T}_2 \dots$ by successive mesh refining using local refinement indicators derived from some η_{xyz} from Section 3.

Algorithm 4.1. *INPUT* coarse mesh \mathcal{T}_0 . For any level $\ell = 0, 1, 2, \dots$ do *COMPUTE* discrete solution u_ℓ on \mathcal{T}_ℓ with $\text{ndof} := |\mathcal{N}_\ell(\Omega)|$ degrees of freedom, error estimator η_{xyz} , efficiency indices $EI := \eta_{xyz}(k) / \|e\|$, and refinement indicators

$$\eta_\ell(T)^2 = \eta_{xyz}(T)^2 + \|h_\xi^{3/2} \partial_\xi^2 u_D / \partial s^2\|_{L^2(\partial T \cap \partial\Omega)}^2.$$

MARK minimal set (for adaptive mesh-refinement) $\mathcal{M}_\ell \subseteq \mathcal{T}_\ell$ of elements such that

$$1/2 \sum_{T \in \mathcal{T}_\ell} \eta_\ell(T)^2 \leq \sum_{T \in \mathcal{M}_\ell} \eta_\ell(T)^2.$$

(For uniform mesh-refinement set $\mathcal{M}_\ell = \mathcal{T}_\ell$.)

REFINE \mathcal{T}_ℓ by *red*-refinement of elements in \mathcal{M}_ℓ and *red-green-blue*-refinement of further elements to avoid hanging nodes and compute $\mathcal{T}_{\ell+1}$.
 od

4.2. Numerical example on L-shaped domain

The first benchmark problem employs $f \equiv 0$ and inhomogenous Dirichlet data u_D of the exact solution

$$u(r, \varphi) = r^{2/3} \sin(2\varphi/3)$$

on the L-shaped domain $\Omega = (-1, 1)^2 \setminus ([0, 1] \times [-1, 0])$. The problem involves a typical corner singularity and shows an empirical convergence rate of $1/3$ for uniform mesh refinement. This can be improved by adaptive refinement as shown in Figure 4. All error estimators induce meshes with the optimal empirical convergence rate 0.5.

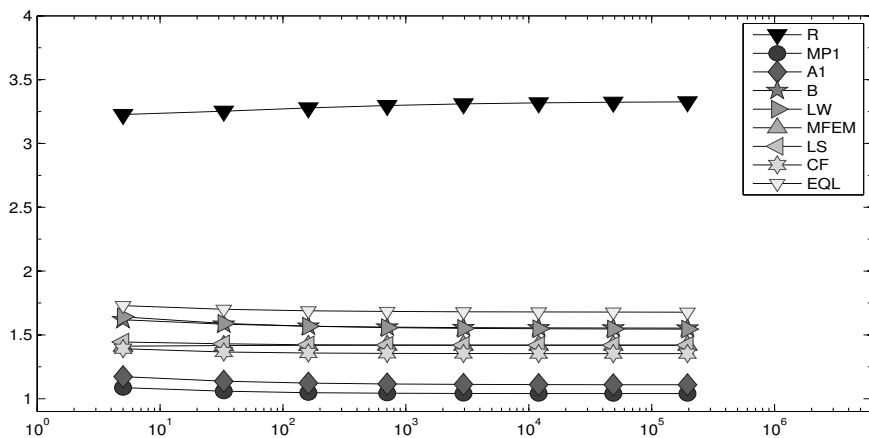


FIGURE 2. History of efficiency indices $\eta_{xyz}/|||e|||$ of various a posteriori error estimators η_{xyz} labelled xyz in the figure as functions of the number of unknowns on uniform meshes in Subsection 4.2.

Figures 2 and 3 display the efficiency indices for uniform and adaptive mesh refinement. The optimal averaging η_{MP1} turns out to be asymptotic exact, but η_{MP1} as well as η_{A1} yield no guaranteed upper bound as the other estimators. While η_R takes efficiency indices of almost 4, all other error estimators arrive at efficiency indices below 1.7. The localisation error estimator η_{CF} is very accurate with values about 1.35 and is only beaten by η_{LW} for adaptive mesh refinement.

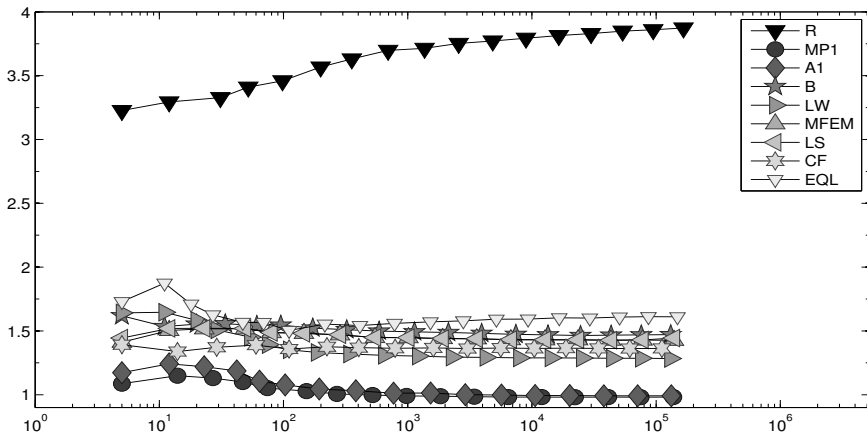


FIGURE 3. History of efficiency indices $\eta_{xyz}/|||e|||$ of various a posteriori error estimators η_{xyz} labelled xyz in the figure as functions of the number of unknowns on adaptive meshes in Subsection 4.2.

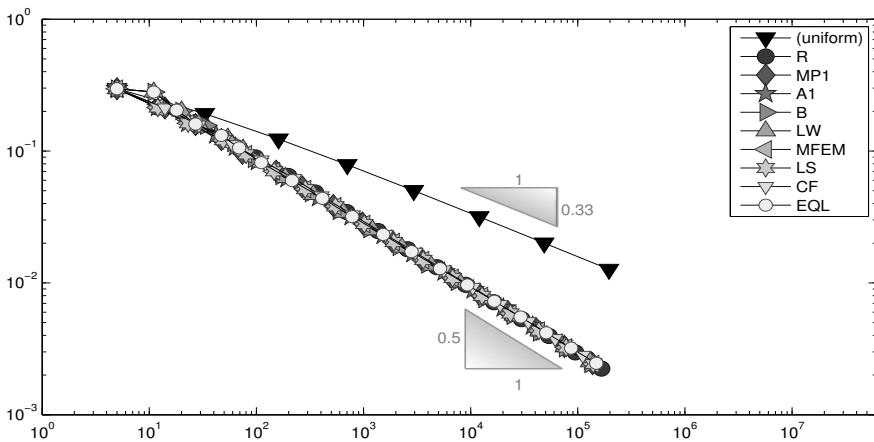


FIGURE 4. Convergence history of the energy error $|||e|||(\eta_{xyz})$ for uniform and adaptive mesh refinement driven by various a posteriori error estimators η_{xyz} as functions of the number of unknowns in Subsection 4.2.

5. Nonconforming finite element method

This section deals with error control for nonconforming approximation for the Poisson model problem.

5.1. Discrete problem and notation

With the elementwise first-order polynomials $P_1(\mathcal{T})$, the nonconforming Crouzeix-Raviart finite element spaces read

$$\begin{aligned} CR^1(\mathcal{T}) &:= \{v \in P_1(\mathcal{T}) \mid v \text{ is continuous at } \text{mid}(\mathcal{E})\}, \\ CR_0^1(\mathcal{T}) &:= \{v \in CR^1(\mathcal{T}) \mid \forall E \in \mathcal{E}(\partial\Omega), v(\text{mid}(E)) = 0.\} \end{aligned}$$

The Crouzeix-Raviart finite elements form a subspaces of the broken Sobolev functions $H^1(\mathcal{T}) := \{v \in L^2(\Omega) \mid \forall T \in \mathcal{T}, v|_T \in H^1(T)\}$ with piecewise gradient $(\nabla_{\text{NC}}v)|_T = \nabla v|_T$ for $v \in H^1(\mathcal{T})$ and $T \in \mathcal{T}$.

5.2. Error control via nonconforming residual

The error control derived in [24] consists of two contributions. The first component contains the right-hand side f and its elementwise oscillations,

$$\text{osc}(f, \mathcal{T}) := \|h_{\mathcal{T}}(f - f_{\mathcal{T}})\|_{L^2(\Omega)},$$

with the piecewise integral mean $f_{\mathcal{T}}$ and the piecewise constant mesh-size $h_{\mathcal{T}}$, $h_{\mathcal{T}}|_T := h_T$ for $T \in \mathcal{T}$. It reads

$$\eta := \|f_{\mathcal{T}}/2 (\bullet - \text{mid}(\mathcal{T}))\|_{L^2(\Omega)} + 1/\pi \text{osc}(f, \mathcal{T}). \tag{5.1}$$

The second component derives from the residual defined, for any test function $v \in H^1(\Omega)$, by

$$\text{Res}_{\text{NC}}(v) := \int_{\partial\Omega} v \partial u_D / \partial s \, ds - \int_{\Omega} \nabla_{\text{NC}} u_{\text{CR}} \cdot \text{Curl } v \, dx.$$

Its dual norm reads

$$\|\|\text{Res}_{\text{NC}}\|\|_{\star} := \sup_{\substack{v \in H^1(\Omega) \\ \text{Curl } v \neq 0}} \text{Res}_{\text{NC}}(v) / \|\text{Curl } v\|_{L^2(\Omega)}.$$

The Helmholtz decomposition allows a split of the error in the broken energy norm

$$\|e\|_{\text{NC}}^2 \leq \eta^2 + \|\|\text{Res}_{\text{NC}}\|\|_{\star}^2.$$

The dual norm $\|\|\text{Res}_{\text{NC}}\|\|_{\star}$ can be estimated with the error estimators from Section 3 with the data $f := 0$ and $\sigma_h := \text{Curl } u_{\text{CR}}$ and Neumann boundary data $g := \partial u_D / \partial s$. On the other hand, there exists an alternative characterisation of $\|\|\text{Res}_{\text{NC}}\|\|_{\star}$,

$$\|\|\text{Res}_{\text{NC}}\|\|_{\star} = \min_{\substack{v \in H^1(\Omega) \\ v = u_D \text{ on } \partial\Omega}} \|u_{\text{CR}} - v\|_{\text{NC}}.$$

Any conforming interpolation $v \in H^1(\Omega)$ with $v = u_D$ on $\partial\Omega$ gives an upper bound for $\|\|\text{Res}_{\text{NC}}\|\|_{\star}$.

5.3. Interpolation after Ainsworth

This subsection introduces the interpolation operator after Ainsworth [1] that designs some piecewise linear $I_A u_{CR} \in H_0^1(\Omega)$ with respect to the original triangulation \mathcal{T} .

$$(I_A v)(z) := \begin{cases} u_D(z) & \text{if } z \in \mathcal{N} \setminus \mathcal{K}, \\ \sum_{T \in \mathcal{T}(z)} u_{CR}|_T(z) / |\mathcal{T}(z)| & \text{if } z \in \mathcal{K}. \end{cases}$$

The error estimator reads

$$\mu_A := \|\nabla_{NC} u_{CR} - \nabla(I_A u_{CR})\|_{L^2(\Omega)}.$$

5.4. Modified interpolation operator

This subsection introduces an improved interpolation operator that designs some piecewise linear $I_{RED} u_{CR} \in H_0^1(\Omega)$ with respect to the red refined triangulation $\text{red}(\mathcal{T})$. The nodes of $\text{red}(\mathcal{T})$ consists of the nodes \mathcal{N} and the edge midpoints $\text{mid}(\mathcal{E})$ of \mathcal{T} . At the boundary the interpolation equals the nodal interpolation of u_D and on all edge midpoints it equals u_{CR} .

$$(I_{RED} v)(z) := \begin{cases} u_{CR}(z) & \text{for } z \in \text{mid}(\mathcal{E}) \setminus \text{mid}(\mathcal{E}(\partial\Omega)), \\ u_D(z) & \text{for } z \in (\mathcal{N} \cup \text{mid}(\mathcal{E})) \cap \partial\Omega, \\ v_z & \text{for } z \in \mathcal{K}. \end{cases}$$

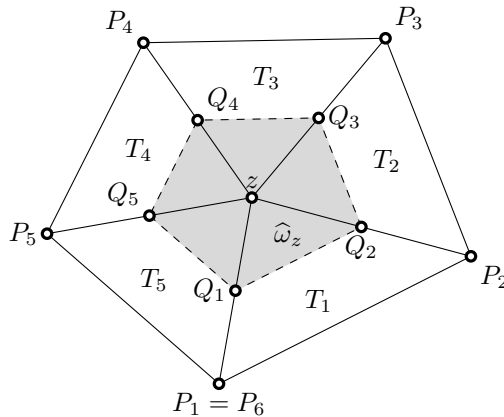


FIGURE 5. Interior patch

In this way, the interpolation equals u_{CR} on all central subtriangles like T_4 in Figure 6 and it remains to determine the values v_z at free nodes $z \in \mathcal{K}$. They may be chosen as in the design of I_A , but we suggest to choose them locally optimal as follows. Consider the node patch $\hat{\omega}_z$ with respect to the red-refined triangulation as in Figure 5. Then minimise the contribution $\|\nabla_{NC} u_{CR} - \nabla v\|_{L^2(\hat{\omega}_z)}$ under the side condition of the fixed values at the

edge midpoints Q_j of the adjacent edges. The value v_z at z remains the only degree of freedom in this local problem. The complete error estimator reads

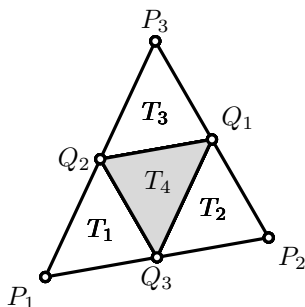


FIGURE 6. Central subtriangle $T_4 = \text{conv}\{\text{mid}(\mathcal{E}(T))\}$ in $\text{red}(T)$ for $T \in \mathcal{T}$.

$$\mu_{\text{RED}} := \|\nabla_{\text{NC}} u_{\text{CR}} - \nabla(I_{\text{RED}} u_{\text{CR}})\|_{L^2(\Omega)}.$$

We distinguish between the optimal version μ_{PMRED} , where v_z is chosen patchwise minimal (PM) as described above, and μ_{MARED} with the suboptimal choice v_z as in Subsection 5.3. This can be seen as a modification of I_A at the edge midpoints.

5.5. Optimal choices

The optimal $v \in P_1(\mathcal{T}) \cap C(\Omega)$ is attained at the solution u_C of the conforming formulation of the Poisson problem, since the nodal basis functions are included in $CR^1(\mathcal{T})$ and hence

$$\begin{aligned} \int_{\Omega} f v \, dx &= \int_{\Omega} \nabla_{\text{NC}} u_{\text{CR}} \cdot \nabla v_C \, dx \\ &= \int_{\Omega} \nabla u_C \cdot \nabla v_C \, dx \quad \text{for all } v_C \in P_1(\mathcal{T}) \cap H_0^1(\Omega). \end{aligned}$$

For comparison, we also compute the optimal $v_{\text{MP1RED}} \in P_1(\text{red}(\mathcal{T})) \cap C(\Omega)$ on the red-refined triangulation $\text{red}(\mathcal{T})$ and the optimal piecewise quadratic $v_{\text{MP2}} \in P_2(\mathcal{T}) \cap C(\Omega)$. Note that they don't have to equal the corresponding conforming solutions. To reduce the computational costs of v_{MP1RED} one might use $I_{\text{MARED}} u_{\text{CR}}$ as an initial guess for some iterative solver to draw near the optimal value. We use a preconditioned conjugate gradients algorithm and stop at the third iterate $v_{\text{MP1RED}(3)}$. For the preconditioner we use the diagonal of the system matrix also known as Jacobi preconditioner.

5.6. Numerical example on L-shaped domain

Recall the data from the L-shaped problem from Section 4.2. Figures 7 and 8 show the efficiency indices of all estimators for uniform and adaptive mesh refinement, respectively. They vary between 1.1 for η_{MP2} and about 1.55 for

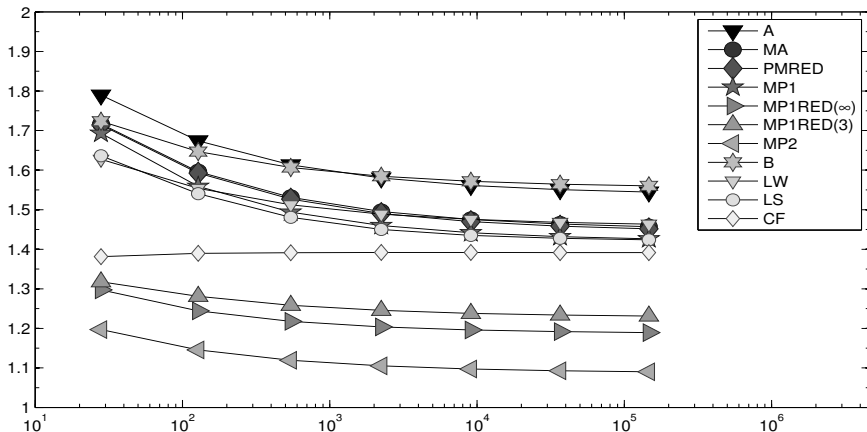


FIGURE 7. History of efficiency indices $\eta_{xyz}/|||e|||$ of various a posteriori error estimators η_{xyz} labelled xyz in the figure as functions of the number of unknowns on uniform meshes in Subsection 5.6.

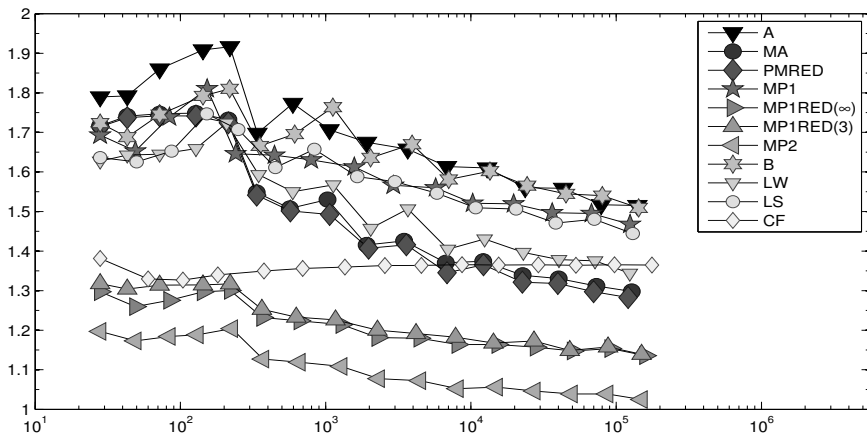


FIGURE 8. History of efficiency indices $\eta_{xyz}/|||e|||$ of various a posteriori error estimators η_{xyz} labelled xyz in the figure as functions of the number of unknowns on adaptive meshes in Subsection 5.6.

η_A or η_B . The improved estimators η_{MARED} and η_{PMRED} perform significantly better. Their overestimation decreases under 35 percent which is even better than η_{MP1} or η_{LS} . The estimator η_{LW} performs similar but slightly worse compared to η_{MARED} . Figure 9 shows the convergence history of the

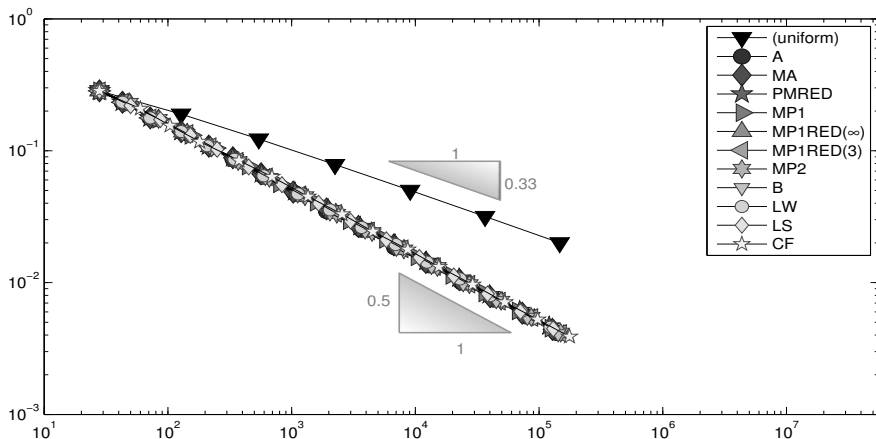


FIGURE 9. Convergence history of the energy error $\|e\|(\eta_{xyz})$ for uniform and adaptive mesh refinement driven by various a posteriori error estimators η_{xyz} as functions of the number of unknowns in Subsection 5.6.

energy error for the adaptive meshes. The quality of the adaptive meshes is comparable for all error estimators.

6. Conforming obstacle problems

The unique exact weak solution $u \in K$ of the obstacle problem inside the closed and convex set of admissible functions,

$$K := \{v \in H^1(\Omega) \mid v = 0 \text{ on } \Gamma_D \text{ and } \chi \leq v \text{ a.e. in } \Omega\} \neq \emptyset$$

satisfies

$$\int_{\Omega} \nabla u \cdot \nabla(u - v) \, dx \leq \int_{\Omega} f(u - v) \, dx \text{ for all } v \in K. \tag{6.1}$$

6.1. Error control via auxiliary residual

After [12] and for a particular choice of Λ_h [23], the discrete solution of the obstacle problem u_h in

$$K(\mathcal{T}) := \{v_h \in P_1(\mathcal{T}) \cap C(\Omega) \mid v_h = 0 \text{ on } \Gamma_D \text{ and } \mathcal{I}\chi \leq v_h \text{ in } \Omega\}$$

solves also the discrete version of the Poisson problem for $w \in V$ with

$$\int_{\Omega} \nabla w \cdot \nabla v \, dx = \int_{\Omega} (f - \Lambda_h)v \, dx \text{ for all } v \in V. \tag{6.2}$$

The associated residual reads, for any $v \in H_0^1(\Omega)$,

$$\text{Res}_{\text{AUX}}(v) := \int_{\Omega} (f - \Lambda_h)v \, dx - \int_{\Omega} \nabla u_h \cdot \nabla v \, dx.$$

The energy norm difference $\|w - u_h\| = \|\text{Res}_{\text{AUX}}\|_*$ between u_h and the exact solution w of the Poisson problem (6.2) can be estimated by any a posteriori error estimator from Section 3. In the conforming case $\chi \leq \mathcal{I}\chi$, [23] leads, for any a posteriori estimator η for $\|w - u_h\|$, to the reliable global upper bound (GUB) in the strict sense of

$$\|e\| \leq \text{GUB}(\eta) := (\eta + \|\Lambda_h - J\Lambda_h\|_*) / 2 + \sqrt{\int_{\Omega} (\chi - u_h) J\Lambda_h \, dx + (\eta + \|\Lambda_h - J\Lambda_h\|_*)^2}.$$

The patchwise oscillations

$$\text{osc}(\Lambda_h, \mathcal{N}) := \left(\sum_{z \in \mathcal{N}} h_z^2 \min_{f_z \in \mathbb{R}} \|\Lambda_h - f_z\|_{L^2(\omega_z)}^2 \right)^{1/2}$$

are a computable bound for

$$\|\Lambda_h - J\Lambda_h\|_* := \sup_{v \in V \setminus \{0\}} \int_{\Omega} (\Lambda_h - J\Lambda_h)v \, dx / \|v\| \lesssim \text{osc}(\Lambda_h, \mathcal{N}).$$

The competition in [23] compares five classes of error estimators from Section 3.

6.2. Numerical example with constant obstacle on L-shaped domain

This benchmark example from [8] mimics a typical corner singularity on the L-shaped domain $\Omega = (-2, 2)^2 \setminus ([0, 2] \times [-2, 0])$ with constant obstacle $\chi = \mathcal{I}\chi \equiv 0$ and homogeneous Dirichlet data $u_D \equiv 0$ along $\partial\Omega$, with the right-hand side

$$f(r, \varphi) := -r^{2/3} \sin(2\varphi/3) (7/3 (\partial g/\partial r)(r)/r + (\partial^2 g/\partial r^2)(r)) - H(r - 5/4),$$

$$g(r) := \max\{0, \min\{1, -6s^5 + 15s^4 - 10s^3 + 1\}\}$$

for $s := 2(r - 1/4)$ and the Heaviside function H . The exact solution reads

$$u(r, \varphi) := r^{2/3} g(r) \sin(2\varphi/3).$$

The experimental convergence rate for uniform refinement is about 0.4 and adaptive refinement improves it to the optimal value 0.5 as depicted in Figure 12. Figures 10 and 11 monitor the efficiency of the upper bounds $\text{GUB}(\eta_{\text{xyz}})$. The efficiency of the bound associated to the standard residual-based error estimator $\text{GUB}(\eta_{\text{R}})$ is between 7 and 9, while all other error estimators allow efficiency indices below 2. As observed in a posteriori error estimation for Poisson Problems in Section 4.2, the upper bound $\text{GUB}(\eta_{\text{MP1}})$ almost arrives at efficiency index 1.

7. Conclusions

The theoretical and practical results of this paper support the following observations.

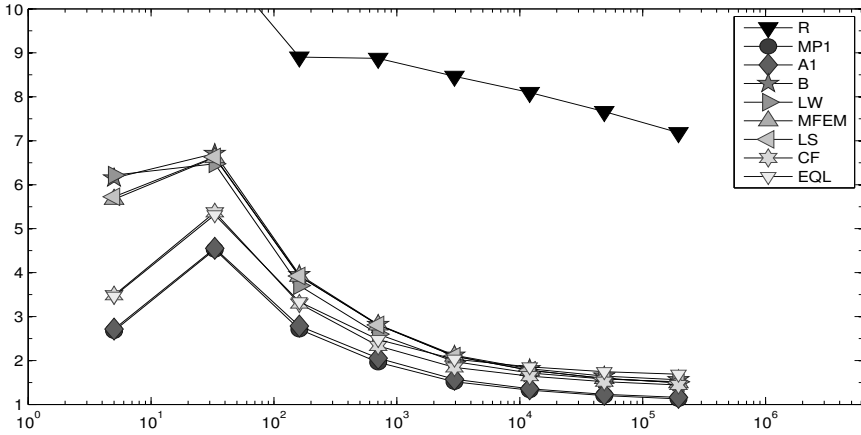


FIGURE 10. History of efficiency indices $GUB(\eta_{xyz})/\|e\|$ of various a posteriori error estimators η_{xyz} labelled xyz in the figure as functions of the number of unknowns on uniform meshes in Subsection 6.2.

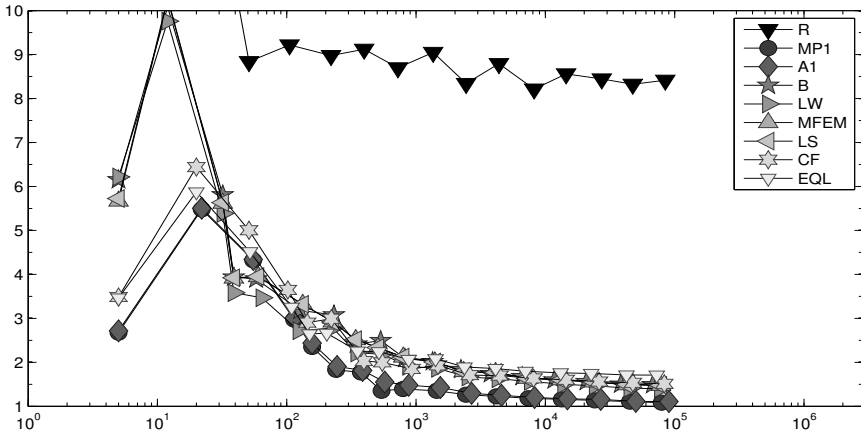


FIGURE 11. History of efficiency indices $GUB(\eta_{xyz})/\|e\|$ of various a posteriori error estimators η_{xyz} labelled xyz in the figure as functions of the number of unknowns on adaptive meshes in Subsection 6.2.

7.1. Explicit error estimators sufficient for effective mesh design

Adaptive mesh refinement may be steered by simple η_R -based refinement rules. It does not appear to be favourable to spend more computational time for more laborious refinement rules if the data are (relatively) smooth.

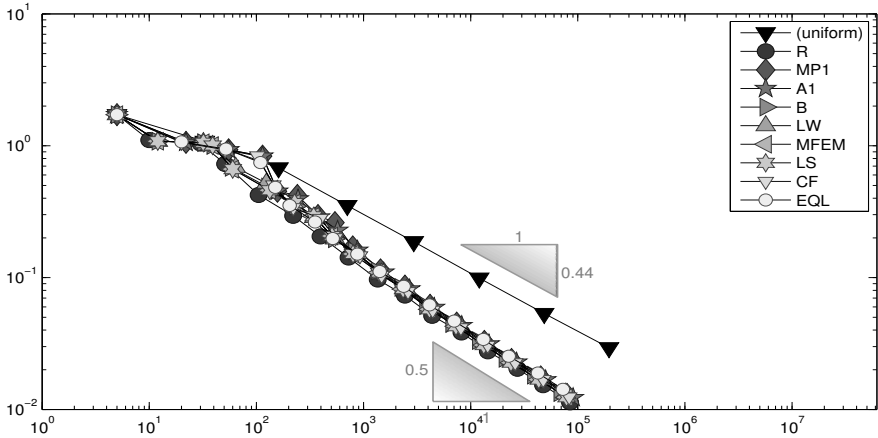


FIGURE 12. Convergence history of the energy error $\|e\|$ for uniform and adaptive mesh refinement driven by various a posteriori error estimators η_{xyz} as functions of the number of unknowns in Subsection 6.2.

7.2. Approximation of local problems

We found that fourth-order polynomials are sufficient enough to provide accurate approximations of the guaranteed upper bounds. However, for full reliability, this approximation error has to be controlled further. The numerical experiments in this paper leave this out and therefore are not fully reliable. This fundamental difficulty is circumvented by modern equilibration error estimators like η_B and η_{LW} . This suffices to conclude, that the novel techniques are superior to η_{EQL} or η_{CF} .

7.3. Robust error control via η_{CF} , η_{LS} , η_{MFEM} or η_{LW}

The estimators η_{CF} , η_{LS} or η_{MFEM} and η_{LW} seem to be the most robust estimators and are recommended as a termination criterion for guaranteed error control. The residual-based estimator η_R is too coarse and not appropriate as termination criterion for guaranteed error control.

7.4. Accurate error control pays off

Averaging error estimators might be an very good exact error guess but they do not guarantee to be an upper bound for the exact error to justify termination. On the other hand, relying only on cheap error estimators like η_R causes overkill refinements and might be more expensive than the computation of more laborious but sharper error estimators like the ones from Section 7.3. That is why it is favorable to have a variety of error estimators [11].

7.5. Recommendation in practise

In the end a combination of several error estimators is recommended, e.g., η_R for generating refinement indicators and a simple averaging error estimator

for the decision whether to refine or to employ a fine error estimator to justify termination or the need for further refinement.

References

- [1] Ainsworth, M., *Robust a posteriori error estimation for nonconforming finite element approximation*, SIAM J. Numer. Anal., **42**(2004), no. 6, 2320-2341.
- [2] Ainsworth, M., Dörfler, W., *Reliable a posteriori error control for nonconformal finite element approximation of Stokes flow*, Math. Comp., **74**(2005), no. 252, 1599-1619 (electronic).
- [3] Ainsworth, M., Oden, J.T., *A posteriori error estimation in finite element analysis*, Wiley, 2000.
- [4] Ainsworth, M., Oden, J.T., *A posteriori error estimators for second order elliptic systems, I, Theoretical foundations and a posteriori error analysis*, Comput. Math. Appl., **25**(1993), no. 2, 101-113.
- [5] Ainsworth, M., Oden, J.T., *A posteriori error estimators for second order elliptic systems, II, An optimal order process for calculating self-equilibrating fluxes*, Comput. Math. Appl., **26**(1993), no. 9, 75-87.
- [6] Ainsworth, M., Oden, J.T., *A unified approach to a posteriori error estimation using element residual methods*, Numer. Math., **65**(1993), 23-50.
- [7] Ainsworth, M., Rankin, R., *Fully computable bounds for the error in non-conforming finite element approximations of arbitrary order on triangular elements*, SIAM J. Numer. Anal., **46**(2008), no. 6, 3207-3232.
- [8] Bartels, S., Carstensen, C., *Averaging techniques yield reliable a posteriori finite element error control for obstacle problems*, Numer. Math., **99**(2004), no. 2, 225-249.
- [9] Bartels, S., Carstensen, C., Dolzmann, G., *Inhomogeneous Dirichlet conditions in a priori and a posteriori finite element error analysis*, Numer. Math., **99**(2004), no. 1, 1-24.
- [10] Bartels, S., Carstensen, C., Jansche, S., *A posteriori error estimates for non-conforming finite element methods*, Numer. Math., **92**(2002), 233-256.
- [11] Bartels, S., Carstensen, C., Klose, R., *An experimental survey of a posteriori Courant finite element error control for the Poisson equation*, Adv. Comput. Math., **15**(2001), no. 1-4, 79-106.
- [12] Braess, D., *A posteriori error estimators for obstacle problems - Another look*, Numer. Math., **101**(2005), 415-421.
- [13] Braess, D., Schöberl, J., *Equilibrated residual error estimator for edge elements*, Math. Comp., **77**(2008), no. 262, 651-672.
- [14] Brandts, J., Chen, Y., Yang, J., *A note on least-squares mixed finite elements in relation to standard and mixed finite elements*, IMA J. Numer. Anal., **26**(2006), no. 4, 779-789.
- [15] Brenner, S.C., Carstensen, C., *Finite element methods*, John Wiley and Sons, 2004.
- [16] Brenner, S.C., Scott, L.R., *The mathematical theory of finite element methods*, Springer-Verlag, 2008.

- [17] Carstensen, C., *Lectures on finite element methods at Yonsei University (Seoul) and Humboldt-Universität zu Berlin*, 2009/2010.
- [18] Carstensen, C., *All first-order averaging techniques for a posteriori finite element error control on unstructured grids are effective and reliable*, Math. Comp., **73**(2004), 1153-1165.
- [19] Carstensen, C., *A unifying theory of a posteriori finite element error control*, Numer. Math., **100**(2005), no. 4, 617-637.
- [20] Carstensen, C., Eigel, M., Hoppe, R.H.W., Löbhard, C., *A review of unified a posteriori finite element error control*, IMA Preprint Series, **2338**(2010).
- [21] Carstensen, C., Funken, S.A., *Fully reliable localised error control in the FEM*, SIAM J. Sci. Comput., **21**(1999), no. 4, 1465-1484 (electronic).
- [22] Carstensen, C., Merdon, C., *Estimator competition for Poisson problems*, J. Comp. Math., **28**(2010), no. 3, 309-330.
- [23] Carstensen, C., Merdon, C., *A posteriori error estimator competition for conforming obstacle problems, part 1: Theoretical preliminaries, part 2: Numerical results*, submitted.
- [24] Carstensen, C., Merdon, C., *Computational survey on a posteriori error estimators for nonconforming finite element methods for the Poisson problem*, in preparation.
- [25] Carstensen, C., Merdon, C., *Six remarks on the Luce-Wohlmuth a posteriori error control* (in preparation).
- [26] Dietrich, B., *Finite elements - Theory, fast solvers, and applications in solid mechanics*, Cambridge University Press, 2007.
- [27] Girault, V., Raviart, P.A., *Finite element methods for Navier-Stokes equations*, Springer-Verlag, 1986.
- [28] Hoppe, H.W., Wohlmuth, B., *Element-oriented and edge-oriented local error estimators for nonconforming finite element methods*, 1996.
- [29] Ladeveze, P., Leguillon, D., *Error estimate procedure in the finite element method and applications*, SIAM J. Numer. Anal., **20**(1983), no. 3, 485-509.
- [30] Luce, R., Wohlmuth, B.I., *A local a posteriori error estimator based on equilibrated fluxes*, Society for Industrial and Applied Mathematics, 2004.
- [31] Marini, L.D., *An inexpensive method for the evaluation of the solution of the lowest order Raviart-Thomas mixed method*, SIAM J. Numer. Anal., **22**(1985), 493-496.
- [32] Payne, L.E., Weinberger, H.F., *An optimal Poincaré inequality for convex domains*, Arch. Rat. Mech. Anal., **5**(1960), 286-292.
- [33] Repin, S., *A posteriori estimates for partial differential equations*, Walter de Gruyter, 2008.
- [34] Repin, S., *Two-sided estimates of deviation from exact solutions of uniformly elliptic equations*, Proceedings of the St. Petersburg Mathematical Society, **IX**(2003), 143-171.
- [35] Repin, S., Sauter, S., Smolianski, A., *A posteriori error estimation for the Dirichlet problem with account of the error in the approximation of boundary conditions*, Computing, **70**(2003), no. 3, 205-233.
- [36] Stoyan, G., *Towards discrete Velle decompositions and narrow bounds for inf-sup constants*, Comput. Math. Appl., **38**(1999), no. 7-8, 243-261.

- [37] Valdman, J., *Minimization of functional majorant in a posteriori error analysis based on $H(\text{div})$ multigrid-preconditioned CG method*, Advances in Numerical Analysis, 2009.
- [38] Verfürth, R., *A posteriori error estimators for the Stokes equations. II, Non-conforming discretizations*, Numer. Math., **60**(1991), no. 2, 235-249.
- [39] Verfürth, R., *A posteriori error estimators for the Stokes equations*, Numer. Math., **55**(1989), no. 3, 309-325.
- [40] Vohralík, M., *Guaranteed and fully robust a posteriori error estimates for conforming discretizations of diffusion problems with discontinuous coefficients*, 2009.
- [41] Volker, J., *A posteriori L_2 -error estimates for the nonconforming P_1/P_0 -finite element discretization of the Stokes equations*, J. Comput. Appl. Math., **96**(1998), no. 2, 99-116.

Carsten Carstensen and Christian Merdon
Humboldt-Universität zu Berlin
Unter den Linden 6
10099 Berlin, Germany

and

Department of Computational Science and Engineering
Yonsei University
120-749 Seoul, Korea
e-mail: cc@mathematik.hu-berlin.de
merdon@mathematik.hu-berlin.de